Chapter 6

Effect of dilution of both A- and B- sites on the multiferroic properties of spinel Mott insulators

6.1 Introduction

As we have discussed the properties of MnV_2O_4 and ZnV_2O_4 in previous chapters of AV_2O_4 series. In this Chapter we are going to discuss about FeV_2O_4, which is a unique compound among such spinel vandium oxides comprising both Fe^{2+} and V^{3+} ions with orbital degrees of freedom; Fe^{2+} ion at the tetrahedral site (A-site) having three 3d electrons in the doubly degenerate e_g states. Very recent development shows structural and magnetic properties of the spinal FeV_2O_4 [1] exhibiting successive structural transitions from cubic to compressed tetragonal with the lattice constants of $c < a$ at $T_{s_1} \sim 140$ K which is due to the cooperative Jahn–Teller effect of FeO_4 and from tetragonal to orthorhombic transition accompanied by a ferrimagnetic transition at $T_{s2} \sim 110$ K, and from orthorhombic to elongated tetragonal with $c > a$ at $T_{s3} \sim 60$ K with decreasing temperature for polycrystalline samples. It has also been reported that the Jahn–Teller effects and the relativistic spin–orbital coupling play an important role in the determination of the orbital states of Fe^{2+} and V^{3+} ions at low temperatures which were concluded with the help of single crystal X-ray diffraction experiments [2]. Recent reports of NMR and neutron diffraction of FeV_2O_4 indicate that its structure is changing to non-collinear ferrimagnetic state at 60 K from collinear state, where the V^{3+} moments become mounted along the {111} directions [3, 4]. This latter transition is marked by a step in magnetization, a peak in heat capacity, an anomaly in the dielectric constant, and the appearance of polarization. It was found that the application of a magnetic field shifts all these signatures associated to T_{s3} to higher temperatures, while it also clearly affects the value of the polarization, revealing a significant magneto electric coupling. It is suggested that the presence of canted spins in the triangular structure below T_{s3} could be responsible for the appearance of ferroelectricity [5].

The AV_2O_4 system also approaches the itinerant-electron limit with decreasing V-V separation [6, 7]. The predicted critical separation for metallic behavior is $R_c = 2.94$ Å [8]. A Recent study on FeV_2O_4 and CoV_2O_4 shows that with increasing pressure the V-V separation decreases and due to which there is a delocalization of charge carriers in FeV_2O_4 and it induces metallic behavior in CoV_2O_4 [9]. The same effect is also shown by chemical pressure by doping Co at the site of MnV_2O_4 [10]. Recently it is shown that in FeV_2O_4,

CoV_2O_4 and MnV_2O_4 the magnetic transition temperature suppressed and activation energy decreases as Zn^{2+} (non magnetic ion) doped at the A site [11-13]. Furthermore, Li^{1+} is also a non magnetic ion and its size is comparable to Mn, Zn, Fe and Co but Li^{1+} has no 3d electron in their outer shell unlike Fe and Co. Therefore, it will be interesting to investigate the magnetic and transport properties by doping Li in FeV_2O_4 at the A site.

Furthermore, soft magnetic materials are center to nearly every aspect of modern electrical and electronics technology because of their ability to concentrate and to shape magnetic flux with great efficiency. The most important characteristics desired for essentially all soft magnetic applications are high saturation induction, high permeability, low coercivity, and low core loss. In this regard these materials are highly important from the application point of view.

In this Chapter, we have investigated magnetic, electrical polarization and transport properties of $Li_xFe_{1-x}V_2O_4$ ($0 \leq x \leq 0.1$) and $Fe(V_{1-x}Cr_x)_2O_4$ ($0 \leq x \leq 0.05$). We found that with increasing the Li and Cr content at Fe (A) and V (B) sites the Ferrimagnetic transition temperature increases, electric polarization temperature remains same with Cr doping and decreases for Li doping and the system moves towards iterant electron limit due to decrease in the V-V distance with Li doping and moves towards more localized behaviour with Cr doping.

6.2 Experimental

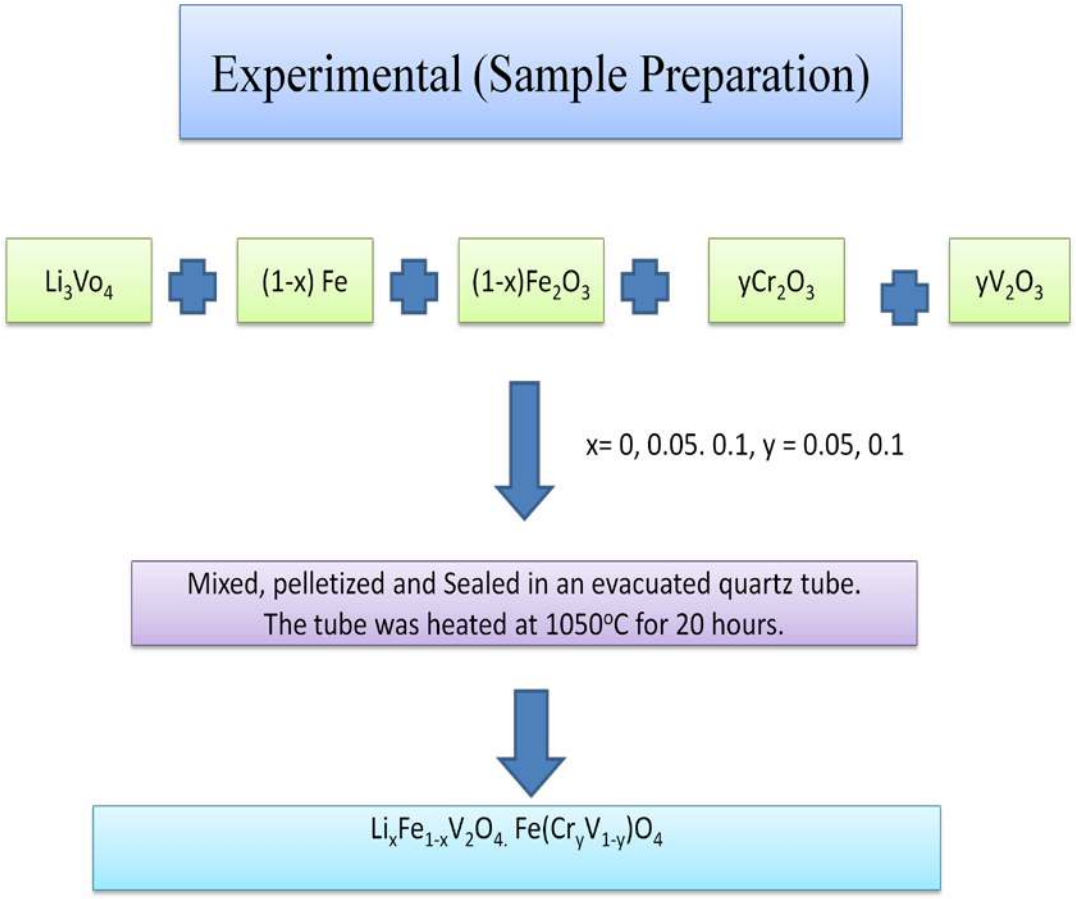

Fig. 6.1. *Block diagram of solid state reaction technique to synthesize $Li_xFe_{1-x}V_2O_4$ and $Fe(Cr_yV_{1-y})O_4$.*

The polycrystalline $Fe(V_{1-x}Cr_x)_2O_4$ $(0\leq x\leq 0.05)$ and $Li_xFe_{1-x}V_2O_4(0\leq x\leq 0.1)$ samples used in this study were prepared by solid state reaction method. Appropriate ratio of Li_3VO_4, Fe, Fe_2O_3, Cr_2O_3, V_2O_3 and V_2O_5 were grounded thoroughly and pressed into pellets. The pellets were sealed in evacuated quartz tube and heated at 1050 ^oC for 20 hours. The X-ray powder diffraction experiment has been performed using Rigaku MiniFlex II DEXTOP X-ray diffractometer with CuKα radiation. Magnetic measurement was done by using MPMS SQUID (Quantum Design) magnetometer with the bulk samples. Ac-susceptibility measurement were done using lock in amplifier SRS830 by homemade setup and standardized with YBCO superconducting sample. The electric polarization (P) as a function of temperature was determined by integrating the pyroelectric

current measured on warming at a rate of 5 K/min with a Keithley 6517A electrometer then cooled with a poling electric field of 640 kV/m applied from 90 K to 6 K. At 6 K, the poling electric field was removed and the electrodes were shortened for 1h to reduce the possible contribution from the detrapped charges. Resistivity measurements have been carried out using four probe method.

6.3 Results and Discussion

6.3.1 Structural analysis

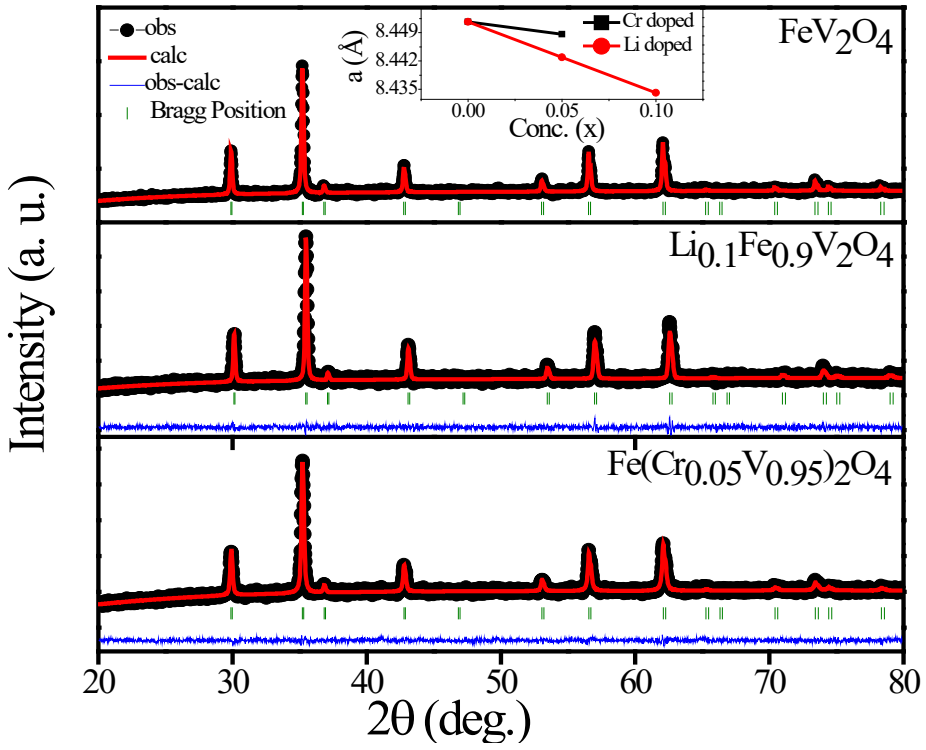

Fig. 6.2. *X-ray diffraction pattern with Rietveld refinement for Li and Cr doped FeV_2O_4 samples at 300 K. The inset shows the variation of lattice parameters with Li and Cr concentration.*

Figure 6.2 shows the X-ray diffraction (XRD) pattern for different Li and Cr doped samples. All peaks are indexed with Fd-3m space group indicating our samples are of pure phase. Inset of the Fig. 6.2 shows variation of lattice parameter with Li and Cr doping, obtained from the Rietveld refinement of the XRD data.

It is observed that with increasing the Li concentration at the Fe site the lattice parameters decrease linearly following the Vegard's law. The same trend is followed by Cr doping also. The ionic size of Li is 0.73Å which is smaller than Fe (0.77Å) and V^{3+} ionic size is 0.78 Å is greater than Cr^{3+} (0.75 Å) ionic radius. As a matter of fact, the lattice parameters decrease with Li and Cr doping. In case of Li doping the lattice parameter decreases very sharply with respect to Cr doping which might be due to the fact that in Li no 3d electrons present in outer shell due to which the Coulomb repulsion decreases between Li/Fe and oxygen 2p electrons. The parameters obtained from Reitveld refinement are given in the Table 6.1.

Table 6.1. *Structural parameters (lattice parameters, bond lengths) of $Fe_{1-x}Li_xV_2O_4$ ($0<x<0.1$) samples obtained from Rietveld refinement of X-ray diffraction data.*

Sample Name	a (Å)	d(V-V) (Å)
FeV_2O_4	8.4517	2.9881
$Fe_{0.95}Li_{0.05}V_2O_4$	8.4429	2.9850
$Fe_{0.9}Li_{0.1}V_2O_4$	8.4341	2.9819
$Fe(Cr_{0.05}V_{0.95})_2O_4$	8.4485	2.9870

6.3.2 Magnetic Property

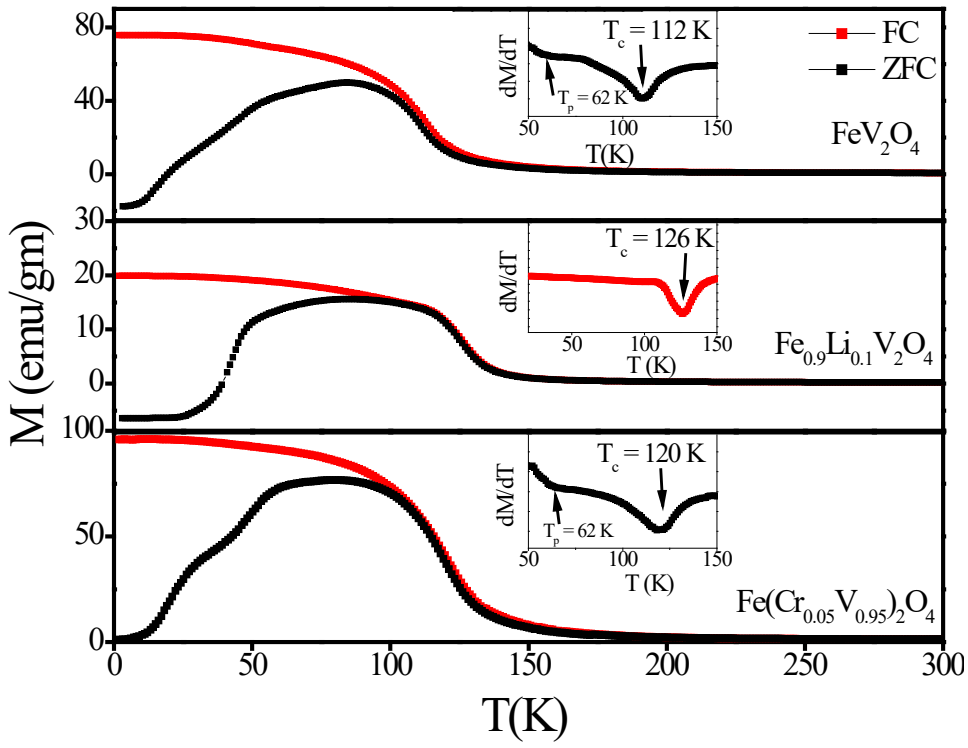

Fig. 6.3. *Temperature variation of magnetization for $Fe_{1-x}Li_xV_2O_4$ [where x=0, 0.05, and 0.1 spinels at H=5000 Oe] and $Fe(Cr_{0.05}V_{0.95})_2O_4$ [where x=0 and 0.05 spinels at H=5000 Oe]. Inset shows the plot of dM/dT vs. T indicating transitions.*

Fig. 6.3 shows the variation of ZFC and FC magnetization with temperature for $Li_xFe_{1-x}V_2O_4$ ($0 \leq x \leq 1$) and $Fe(V_{1-x}Cr_x)_2O_4$ ($0 \leq x \leq 0.05$). For FeV_2O_4 (Fig. 6.3), with decrease of temperature, a transition from paramagnetic (PM) to ferrimagnetic (FI) phase occurs below Tc. ZFC magnetization bifurcates from FC magnetization around 112 K, then decreases with further decreasing temperature. A small rise in FC curve exists at a lower temperature Tp, accompanied by a slight drop in ZFC magnetization. This magnetization behavior is consistent with that already reported [14]. The values of Tc and Tp determined from the dM/dT vs. T curve of the FC magnetization are 112 K and 62 K, respectively. With Li 10% doping the T_C increases to 126 K but the T_P disappears whereas for 5% Cr doping T_C increases to 120 K but T_P remains unchanged. We have also measured ac-susceptibility at 100 Hz for $Li_xFe_{1-x}V_2O_4$ ($0 \leq x \leq 1$) which is shown in Fig. 6.4. Similar behavior is observed that with increasing Li content at A site the ferrimagnetic transition

temperatures increase. This might be due to the fact that shrinkage of the lattice parameter with Li and Cr doping, increases the exchange interaction between the A^{2+} and V^{3+} through oxygen which enhances the ferrimagnetic ordering temperature.

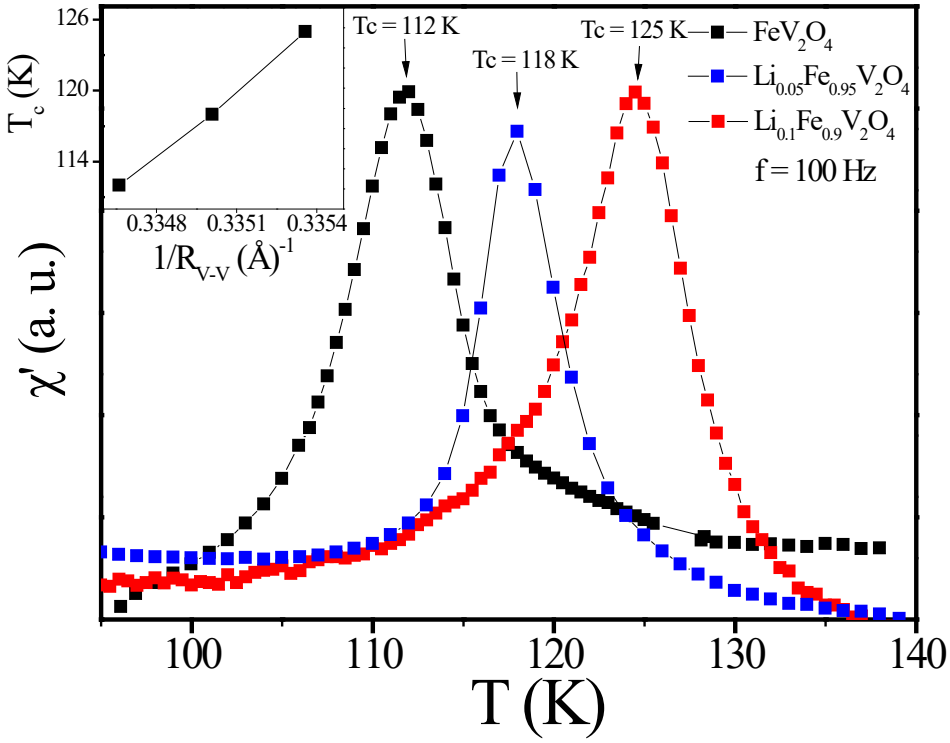

Fig. 6.4. *Temperature dependence of AC magnetization measured in fields with 100 Hz frequency for $Fe_{1-x}Li_xV_2O_4$ [where x=0, 0.05, and 0.1] around T_C. Inset shows the Variation of T_C with respect to $1/R_{V-V}$.*

Fig. 6.5 shows the M(H) curve at 2 K for undoped and Li and Cr doped samples. For the undoped sample a jump at ~0 T and another jump ~1.25 T are observed which are consistent with that reported by Nishihara *et al.* [14]. But when Li is doped the jumps disappear. On the other hand when Cr is doped the 0 T jump shifts to 1.0 T and the 1.25 T jump shifts to 1.3 T and an extra jump is observed at ~2.5 T. In their paper Nishihara *et al.* [14] explained the 1.2 T jump in FeV_2O_4 as the avalanche behavior [15]. But the origin of jumps in Cr doped sample are not yet clear. It might be due to some Martensitic transition [16]. It deserves further study.

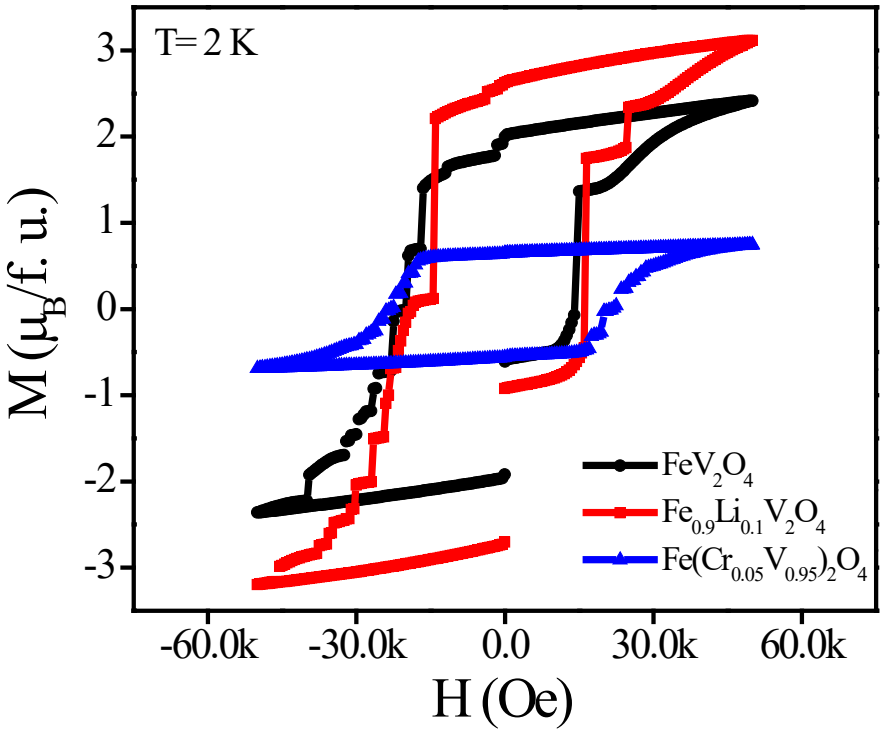

Fig. 6.5. *The isothermal field dependence of the magnetization at 2 K for $Fe_{1-x}Li_xV_2O_4$ [where x=0 and 0.01] and $Fe(Cr_{0.05}V_{0.95})_2O_4$[where x=0.05].*

On the other hand, the saturated moment, estimated from Fig. 6.5, is decreased upon Li doping and is increased for Cr doping. Since Li ions are non-magnetic and Cr ions are more magnetic than V ions and it is known that V spins tend to align anti-parallel to each other when the coupling between A and B sub-lattices is absent. Therefore, the moment of the V sub-lattice also decreases with increasing Li content and increases for Cr content. It is important to compare these with the earlier studies on $Zn_xMn_{1-x}V_2O_4$ [13] and $Co_{1-x}Zn_xV_2O_4$ [12] as Zn (0.74 Å) is also a non magnetic ion. Moreover, the sizes of Li (0.73 Å), Co (0.72 Å) and Zn (0.74 Å) are comparable. In fact, when non-magnetic ion is doped (with ion of lower ionic radius than the A-site ion) two cases arise, the decrease of lattice parameters due to which the V-V distance is reduced resulting the increase of coupling between A and V sites which tries to increase the magnetic transition temperature. Moreover, doping of non magnetic ion at A site decreases the A-V coupling due to which V-V spins try to align anti-paralleled. As a result, the magnetic transition is suppressed.

When Li is doped (in the present investigation) the later one is dominating over the former. But when Zn is doped the former one is dominating over the later [13].

6.3.3 Ferroelectric property

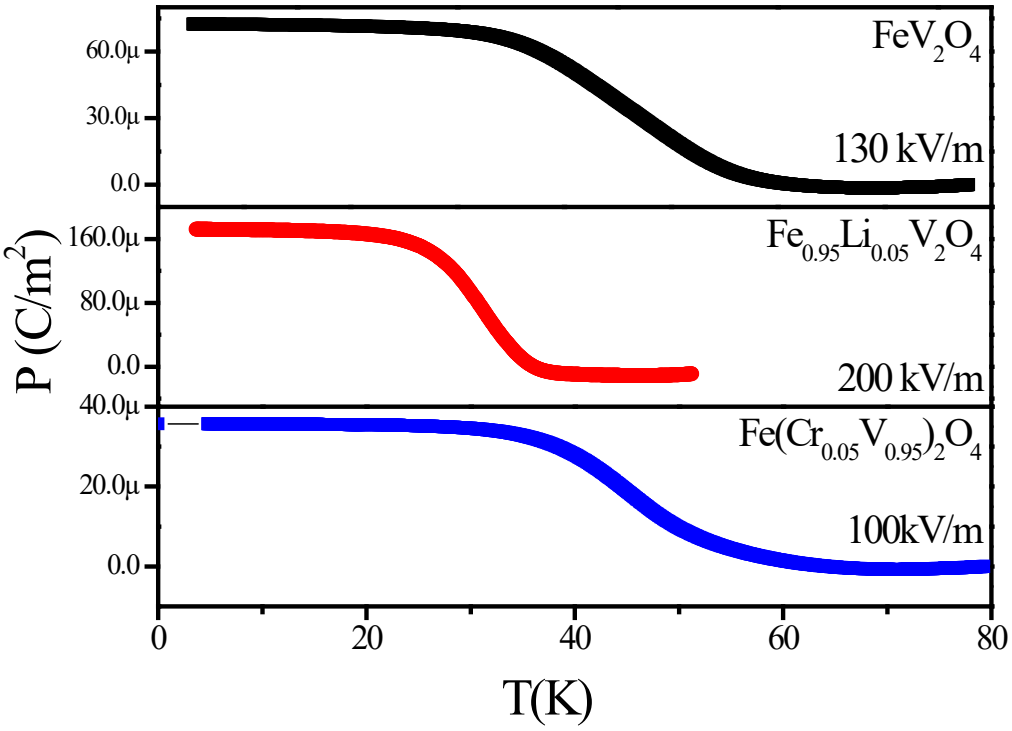

Fig. 6.6. *The temperature dependence of ferroelectric polarization of Li and Cr doped FeV_2O_4.*

Fig. 6.6 shows the temperature dependent electrical polarization for the FeV_2O_4, $Li_{0.05}Fe_{0.95}V_2O_4$ and $Fe(Cr_{0.05}V_{0.95})_2O_4$ samples. The electrical polarization (P) appears at about T_p = 61 K for FeV_2O_4 and 38 K for $Li_{0.05}Fe_{0.95}V_2O_4$ and approaching a saturated value with decreasing temperature. For 10% Li doping no polarization is observed consistent with the magnetization behavior. With Li doping, also the onset temperature decreases. This result emphasizes that this substituted FeV_2O_4 remains a multiferroic until dilution becomes too detrimental to the magnetic ordering. But with Cr doping the onset temperature remains same. In contrast, for the Cr doped samples [$Fe(Cr_{0.05}V_{0.95})_2O_4$], the P(T) curves reveal unchanged T_P (ferroelectric transition temperature) values as x increases. The temperature, T_P, is not changing with Cr content, but the P value decreases

with increase of Cr content. It is thus reasonable to ascribe the polarization origin to the presence of almost non-substituted regions (with compositions near FeV_2O_4 and whose amount decreases with increasing x). From above discussion it is clear that Li doping suppresses the collinear to non collinear state but Cr doping does not change the collinear state to non collinear state, which might be due to the fact that with Li doping the coupling between V-V decreases due to the presence of V^{3+} and V^{4+} at the octahedral site but Cr 5% doping has no effect on V-V coupling which in effect does not change the onset temperature.

6.3.4 Transport properties

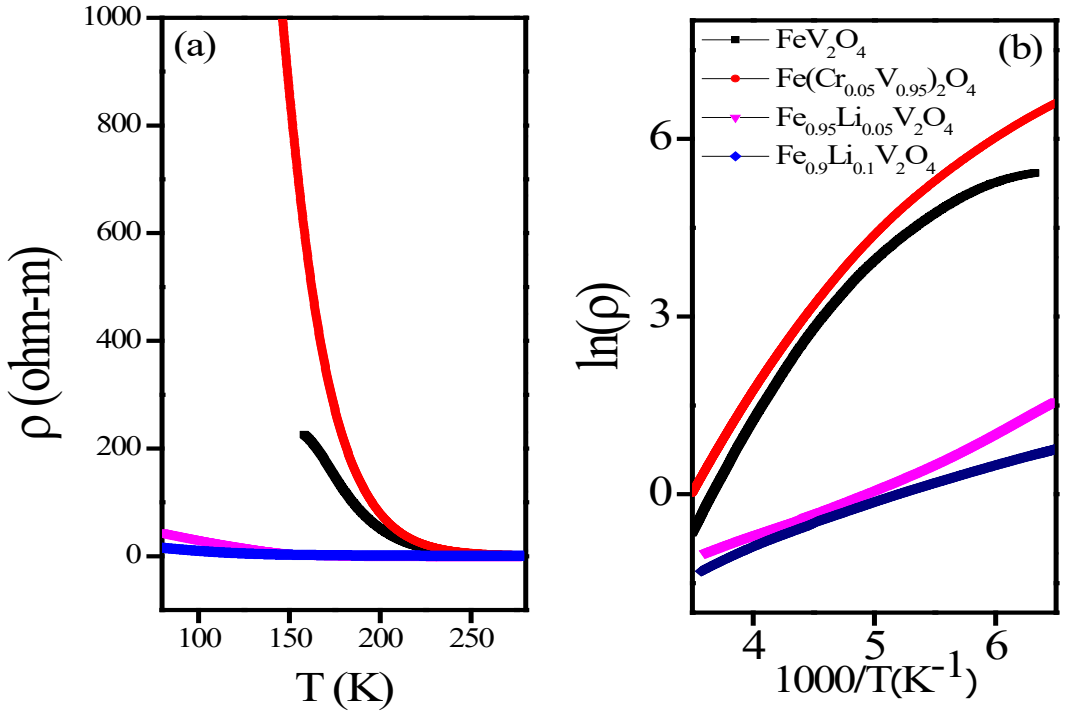

Fig.6.7. *(a) The temperature dependences of resistivity for $Fe_{1-x}Li_xV_2O_4$ [where x=0 and 0.01] and $Fe(Cr_{0.05}V_{0.95})_2O_4$ [where x=0.05] (b) ln ρ vs 1000/T for $Fe_{1-x}Li_xV_2O_4$ [where x=0 and 0.01] and $Fe(Cr_{0.05}V_{0.95})_2O_4$ [where x=0.05].*

Fig. 6.7(a) shows the variation of resistivity with temperature for all the samples and Fig. 6.7(b) shows the ln ρ *vs* 1000/T for $Fe_{1-x}Li_xV_2O_4$ [where x=0 and 0.1] and

$Fe(Cr_{0.05}V_{0.95})_2O_4$ (where x=0.05). As FeV_2O_4 belongs to Mott Insulator regime therefore from the figure it can be mentioned that with increasing Li content at the A site the system moves towards itinerant electron side along with the decrease of V-V distance. The 3*d* electrons in Cr ions are well localized. Therefore, in the Cr doped samples the electrical resistivity shows an insulating behavior.

6.4 Conclusion

The structural, magnetic, electrical and transport properties of FeV_2O_4, by diluting A-site by Li ion and B-site by Cr ion, have been studied. It is observed that increasing the Li content at A site the V-V distance is decreased and due to that ferrimagnetic ordering temperature is increased while the ferroelectric transition temperature is reduced and the whole system moves towards the itinerant electron behavior. In the case of Cr doping the magnetic transition temperature is increased but there is no effect on the ferroelectric transition temperature and the system moves towards more inside the Mott insulating region. So by tuning the V-V distance either by external pressure or chemical pressure we can tune the magnetic, ferroelectric and transport properties or more specifically, the multiferroic properties of Mott-insulating FeV_2O_4 which is very important from the application point of view.

References

[1]. Johnston, D. C., Swenson, C .A. and Kondo, S., Specific heat (1.2–108 K) and thermal expansion (4.4-297 K) measurements of the 3d heavy- fermion compound LiV_2O_4, Phys. Rev. B, 59, 2627-2641, 1999.

[2]. Nii, Y., Sagayama, H., Arima, T., Aoyagi, S., Sakai, R., Maki, S., Nishibori, E., Sawa, H., Sugimoto, K., Ohsumi, H. and Takata, M. , Orbital structures in spinel vanadates AV_2O_4 (A = Fe, Mn) Phys. Rev. B, 86, 125142/1-125142/8, 2012.

[3]. MacDougall, G. J., Garlea, V. O., Aczel, A. A., Zhou, H. D. and Nagler, S. E., Magnetic order and ice rules in the multiferroic spinel FeV_2O_4 Phys. Rev. B, 86, 060414/1-060414/5, 2012.

[4]. Katsufuji, T., Suzuki, T., Takei, H., Shingu, M., Kato, K., Osak, K., Takata, M., Sagayama, H. and Arima, T., Structuaral and Magnetic Properties of spinel FeV_2O_4 with two ions having orbital degree of freedom, J. Phys. Soc. Japan, 77, 053708, 2008.

[5]. Liu, N., Zhao, K. H., Shi, X. L. and Zhang, L. W., Fe^{3+} doping effects on the structure and multiferroicity of $Fe_{1+x}V_{2-x}O4$ ($0 \leq x \leq 0.4$) spinels , J. App. Phys., 111 ,124112/1-124112/5., 2012.

[6]. Rogers, D. B., Arnott, R. J., Wold, A., Goodenough, J. B., The preparation and Properties of Some Vanadium Spinels, J. Phys. Chem. Solids, 24, 347-360, 1963.

[7]. Rogers, D. B., Goodenough, J. B. and Wold, A., Electrical Conductivity in the Spinel System $Co_{1-x}Li_xV_2O_4$., J. Appl. Phys., 35, 1069-1070, 1964.

[8]. Goodenough, J. B., Metallic Oxides, edited by Reiss H, Progress in Solid State Chemistry, Pergamon, New York, Vol. 5, 1972.

[9]. Kismarahardja, A., Brooks, J. S., Kiswandhi, A., Matsubayashi, K., Yamanaka, R., Uwatoko, Y., Whalen, J., Siegrist, T. and Zhou, H. D., $Co[V_2]O_4$: A Spinel Approaching the Itinerant Electron Limit, Phys. Rev. Lett., 106, 056602/1- 056602/4, 2011.

[10]. Kiswandhi, A., Brooks, J. S., Lu, J., Whalen, J., Siegrist, T. and Zhou, H. D., Chemical pressure effects on structural, magnetic, and transport properties of $Mn_{1-x}Co_xV_2O_4$, Phys. Rev. B, 84, 205138/1-205138/7, 2011.

[11]. Ishibashi, H. and Kitadai, Y., Structural and Magnetic Properties in Spinel Type $Fe_{1-x}Zn_xV_2O_4$, Journal of Physics: Conference Series, 391, 012092/1-012092/4, 2012.

[12]. Huang, Y., Yang, Z. and Zhang, Y., Formation and Partial melting of two types of spin- cluster glass behaviour in vanadate spinel, J. Phys.: Condens. Matter, 24, 056001/1-056001/8, 2012.

[13]. Shahi, P., Kumar, A., Sharma, N., Singh, R, Sastry, P. U., Das, A., Kumar, A., Shukla, K. K, Ghosh, A. K., Nigam, A. K. and Chatterjee, S., Effect of dilution of both A- and B- sites on the multiferroic properties of spinal Mott insulators, J. Mater. Sci., 49, 7317, 2014.

[14]. Nishihara, S., Doi, W., Ishibashi, H., Hosokoshi, Y., Ren, X. M. and Mori, S., Appearance of magnetization jumps in magnetic hysteresis curves in spinel oxide FeV_2O_4, J. App. Phys., 107, 09A504/1-09A504/3, 2010.

[15]. Takeda, K., Awaga, K., Inabe, T., Môri, N. and Nojiri, H., Magnetic anisotropy, tunnelling effects, high-frequency EPR, and molecular structure of fast-relaxation species of Mn_{12}, Phys. Rev. B, 65 , 094424/1- 094424/12, 2002.

[16]. Taran, S., Chaudhuri, B. K., Das, ,A., Nigam, A. K., Kremer, R. K. and Chatterjee, S., CE-type antiferromagnetic ordering and martensitic transition in Pr-substituted $La0.65Ca_{0.35}MnO_3$ from magnetic and neutron diffraction studies, J. Phys.: Condens. Matter, 19, 216217/1-216217/8, 2007.